*Journal of Natural Products*
*Vol. 49, No. 3, pp. 475-482, May-Jun 1986*



# TANDEM MASS SPECTROMETRY OF MAYTANSINOIDS

RONALD D. PLATTNER and RICHARD G. POWELL

*Northern Regional Research Center, Agricultural Research Service, U.S. Department of Agriculture,*[1] *Peoria, Illinois 61604*

ABSTRACT.—The positive and negative chemical ionization mass spectra of a series of maytansinoids have been recorded. Unlike electron ionization, in the chemical ionization spectra the high mass ions that are indicative of structure are abundant. Collision activated decomposition produced daughter ions that could be used to confirm proposed structures of characteristic positive and negative ions. Daughter spectra were useful to differentiate structurally similar isomers that had nearly identical mass spectra. Ms/ms scans were also used to identify three new maytansinoids that were present as minor components in some of the reference standards. Using parent scans, maytansinoids were detected at low levels in simple extracts of *Actinosynnema pretiosum* fermentation beers with no sample clean-up.

Maytansinoids have generated considerable research interest because they possess a range of biological activity, including potent antitumor activity. Numerous compounds with this ansamacrolide ring structure have been isolated from higher plants and microbial sources and characterized. The isolation, chemistry, and biological activity of these compounds have been reviewed (1-3).

Electron ionization mass spectra (eims) of maytansinoids usually do not give molecular ions. However, in this mode, these compounds do yield fragments that provide structural information. Each maytansinoid shows a fragment at $(M-61)^+$ [hereafter referred to as $(M-a)^+$] due to the loss of HCNO and $H_2O$ from the cyclic carbamate (3). Compounds with an ester at C-3 (see structures) show an additional fragment ion arising from the loss of that side chain as ROH $[M-(a+b)]^+$. These fragments are typically of quite low abundance, and most of the ion current is carried by low mass fragments that are of little diagnostic use. The extensive fragmentation precludes eims from being a useful technique in directing isolation of or identifying minor maytansinoid components in mixtures of partially refined extracts. Hence, in most of the published data, eims of maytansinoids were used to confirm structure and determine elemental compositions of ei fragments of isolated maytansinoids.

By contrast, cims provides much less fragmentation and produces abundant fragments at higher molecular weight (4). These higher mass ions are ideal candidates for tandem ms/ms studies. Ms/ms, a hyphenated technique developed over the past de-

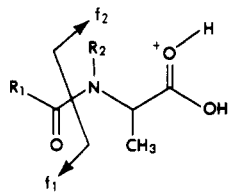


| Compound | | $R_1$ | $R_2$ | $f_1$ | $f_2$ | $f_3$* |
|---|---|---|---|---|---|---|
| **1** | Maytansine | $CH_3$ | $CH_3$ | 43 | 104 | 58 |
| **2** | Maytanprine | $C_2H_5$ | $CH_3$ | 57 | 104 | 58 |
| **9** | Demethyltrewiasine | $C_2H_5$ | H | 43 | 90 | 44 |

*$Hf_2-46=f_3$

[1]The mention of firm names or trade products does not imply that they are endorsed or recommended by the U.S. Department of Agriculture over other firms or similar products not mentioned.

cade, has become an important analytical tool for "needle-in-a-haystack" analytical problems. The technique has been applied to the detection of numerous natural products in plant materials, particularly alkaloids (5), and developments in this field have been reviewed (6,7). This paper reports ms/ms analysis of the characteristic maytansinoid cims ions and uses ms/ms parent and daughter scans to differentiate structurally similar isomers, with similar mass spectra, and to identify maytansinoids directly in complex mixtures.

## RESULTS AND DISCUSSION

Most of the ions formed by maytansinoids in positive and negative ci arise from protonation reactions and resonance and dissociative electron capture reactions. These processes occur simultaneously with either positive or negative ions being selected by proper choice of source biasing. Resulting ions with sufficient excess energy may fragment. Products of protonation are generally even electron ions, and they tend to be more stable than the odd electron radical ions formed in eims. Therefore, fragmentation usually tends to involve the loss of neutral molecules.

With isobutane reagent gas, protonated molecules are not observed among the positive ions from those maytansinoids having nitrogen containing esters at C-3. Table 1 lists the major positive ci fragments for several representative maytansinoids (**1-13**,**16**,**17**). The spectrum of maytansine (**1**) is typical of these spectra. The base peak in the spectrum is due to $(MH\text{-}a)^+$ at *m/z* 631. The next most abundant intense high-mass fragment indicative of structure is at *m/z* 486. It arises from $(MH\text{-}a)^+$ by loss of a neutral acid molecule from the ester side chain at C-3 to yield $[MH\text{-}(a+b)]^+$. Two abundant fragments from the C-3 side chain are also observed. The protonated side chain $bH^+$ is at *m/z* 146, and an ion $(bH\text{-}18)^+$ at *m/z* 128 arises from the acyl group of the side chain. Together, these four fragments account for the bulk of the total ionization.

The two examples with simple, nonnitrogen-containing esters at C-3 both show prominent protonated molecules in positive ci. Ansamitocin P-3 (**16**) shows this protonated molecule at *m/z* 635. Prominent fragments for $(MH\text{-}a)^+$ and $(MH\text{-}a\text{-}b)^+$ are observed, but the ions from the C-3 side chain are not observed.

For most of the maytansinoids low abundance molecular anions are found among the negative ions from isobutane ci (Table 2). Only the ansamitocins, with nitrogen-

TABLE 1. Major Ions and Relative Intensities Observed in Positive cims of Maytansinoids

| | Compound | MW | $(MH\text{-}a)^+$ | $(MH\text{-}a\text{-}b)^+$ | $bH^+$ | $(bH\text{-}18)^+$ |
|---|---|---|---|---|---|---|
| **1** | maytansine | 691 | 631(100) | 486(60) | 146(100) | 128(95) |
| **2** | maytanprine | 705 | 645(20) | 486(40) | 160(100) | 142(45) |
| **3** | maytanbutine | 719 | 659(17) | 486(15) | 174(80) | 156(100) |
| **4** | maytanvaline | 733 | 673(50) | 486(85) | 188(80) | 170(100) |
| **5** | colubrinol | 735 | 675(45) | 501(48) | 174(100) | 156(90) |
| **6** | trewiasine | 749 | 689(30) | 516(30) | 174(90) | 156(100) |
| **7** | 10-epitrewiasine | 749 | 689(18) | 516(21) | 174(100) | 156(30) |
| **8** | dehydrotrewiasine | 747 | 687(60) | 516(53) | 172(100) | 154(95) |
| **9** | demethyltrewiasine | 735 | 675(43) | 516(53) | 160(100) | 142(75) |
| **10** | nortrewiasine | 735 | 675(40) | 502(35) | 174(100) | 156(85) |
| **11** | treflorine | 749 | 689(100) | — | — | — |
| **12** | trenudine | 765 | 705(100) | — | — | — |
| **13** | *N*-methyltrenudone | 777 | 717(100) | — | — | — |
| **16** | ansamitocin P-3 | 634[a] | 574(100) | 486(20) | — | — |
| **17** | ansamitocin P-4 | 648[b] | 588(100) | 486(2) | — | — |

[a]$MH^+$ 635(30).
[b]$MH^+$ 649(32).

TABLE 2. Major Ions and Relative Intensities Observed in Negative cims of Maytansinoids

| | Compound | $M^-$ | $(M\text{-}a)^-$ | $(M\text{-}a\text{-}b)^-$ | $(M\text{-}a\text{-}b\text{-}HCl)^-$ | $(b\text{-}h)^-$ |
|---|---|---|---|---|---|---|
| **1** | maytansine | 691(2) | 630(100) | 485(35) | 449(39) | 144(52) |
| **2** | maytanprine | 705(2) | 644(100) | 485(31) | 449(42) | 158(63) |
| **3** | maytanbutine | 719(3) | 658(100) | 485(31) | 449(27) | 172(70) |
| **4** | maytanvaline | 733(6) | 672(100) | 485(33) | 449(50) | 186(51) |
| **5** | colubrinol | 735(4) | 674(100) | 501(79) | 465(60) | 172(49) |
| **6** | trewiasine | 749(4) | 688(85) | 515(31) | 479(43) | 172(100) |
| **7** | 10-epitrewiasine | 749(4) | 688(100) | 515(3) | 479(45) | 172(10) |
| **8** | dehydrotrewiasine | 747(3) | 686(100) | 515(18) | 479(25) | 170(17) |
| **9** | demethyltrewiasine | 735(1) | 674(100) | 515(14) | 479(29) | 158(25) |
| **10** | nortrewiasine | 735(1) | 674(59) | 501(100) | 466(30) | 172(23) |
| **11** | treflorine | 749(2) | 688(100) | — | — | — |
| **12** | trenudine | 765(1) | 704(100) | — | — | — |
| **13** | *N*-methyltrenudone | 777(1) | 716(100) | — | — | — |
| **16** | ansamitocin P-3 | 634(60) | 573(100) | 485(15) | 449(40) | — |
| **17** | ansamitocin P-4 | 648(69) | 587(100) | 485(25) | 449(52) | 101(30) |

free esters at C-3, show abundant molecular anions. Again the spectrum of maytansine (**1**) is typical and is discussed in detail. The base peak due to the $(M\text{-}a)^-$ anion is at *m/z* 630. The anion of the C-3 ester is observed as an intense fragment $(b\text{-}H)^-$ at *m/z* 144. The loss of the neutral acid at C-3 from the $(M\text{-}a)^-$ is observed to give an ion at *m/z* 485 $[M\text{-}(a+b)]^-$. An additional fragment from $(M\text{-}a)^-$ at *m/z* 449 arises from loss of HCl, and a small fragment (<5% of the base peak) resulting from the attachment of HCl to the (b-H) ion is seen at *m/z* 180.

Both positive and negative ci spectra of maytansinoids are more useful than ei spectra because the structurally important ions are abundant in the ci spectra, accounting for most of the ion current. Inasmuch as the overall sensitivity for the three ionization modes is roughly the same for maytansinoids, identifications can be made with much smaller samples by using the ci technique. For example, more than a microgram of sample is needed to detect even the low abundance fragments at $(M\text{-}a)^+$ and $[M\text{-}(a+b)]^+$ in eims. The analogous ions are abundant in ci spectra being clearly detected in full scan spectra of as little as 1 ng of a pure maytansinoid. Much additional information, for structural confirmation, is available by using ms/ms experiments on these higher mass ci ions.

The ms/ms daughter spectrum of the molecular anion (negative ci) of maytansine is shown in Figure 1. Abundant daughters are seen for the C-3 side-chain anion (*m/z* 144) and for the loss of the side-chain (*m/z* 547). The absence of a daughter at *m/z* 630 probably indicates that the ions at *m/z* 630 in negative ci and *m/z* 631 in positive ci arise from either dissociative electron capture or thermal decomposition of the molecule, as it elutes from the probe, rather than as fragments from the molecular anion or protonated molecule.

The ms/ms daughter spectra of the $(MH\text{-}a)^+$ ions in the maytansinoids also give daughters indicative of the C-3 side chain and the macrolide ring (Table 3). In maytansine, these two ions, $(bH\text{-}18)^+$ at *m/z* 128 and $(MH\text{-}a\text{-}b)^+$ at *m/z* 486, account for over 95% of the total daughter fragments.

Daughter spectra of the $(M\text{-}a)^-$ ions are more complex than the $(MH\text{-}a)^+$ (Table 4). The anion from the side-chain ester $(b\text{-}H)^-$ is the most abundant daughter in all maytansinoids examined. The anion $(M\text{-}a\text{-}b)^-$ is also observed, but its abundance is variable. These two daughter fragments can be used to determine the nature of the side-chain. Other fragments observed include those arising from additional losses of HCl or MeOH from the parent. Additionally, a weak signal is seen in all maytansinoid $(M\text{-}a)^-$

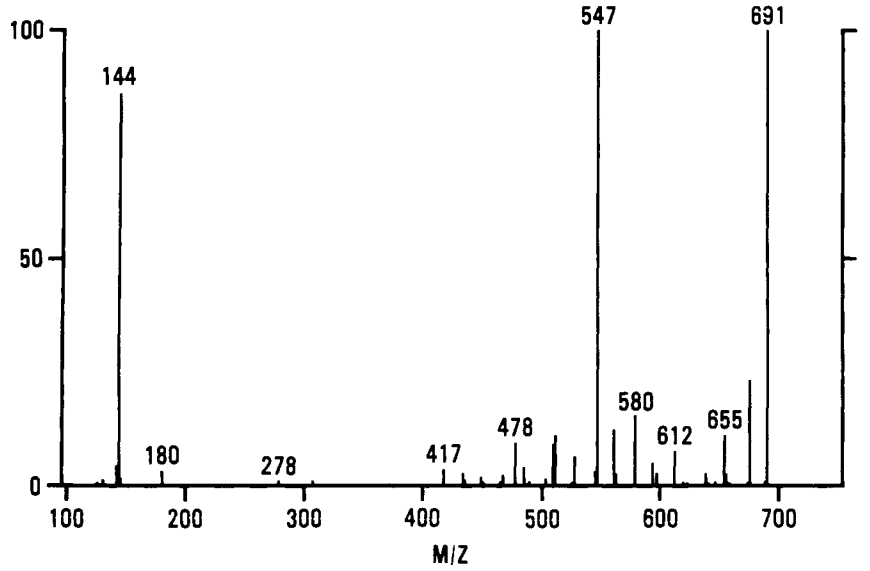


FIGURE 1. Ms/ms daughter spectrum of the molecular anion (*m/z* 691) for maytansine.

daughter spectra at $bCl^-$, which arises from migration of the Cl atom to the ester and fragmentation. This is observed at *m/z* 180 in maytansine.

The structure of the ester side chain can be determined directly from the intact maytansinoid molecule by using ms/ms techniques. Daughter spectra of the protonated C-3 acid and the C-3 acyl side chain for several maytansinoids are given in Tables 5 and 6. Several maytansinoids have side chains with equivalent molecular weights but different structures. For example, the protonated acid side chain ion for maytanprine (**2**) and demethyltrewiasine (**9**) are both observed at *m/z* 160. The nitrogen group of the side chain in maytanprine is methylated, while the side chain of demethyltrewiasine is not. Three primary daughter fragments are observed in the ms/ms spectra of the $bH^+$ ion. Cleavage between the nitrogen and carbonyl forms the acyl ion (at *m/z* 57 in maytanprine and 71 in demethyltrewiasine). Loss of the end group R1 (Scheme 1), with a hydrogen transfer (*m/z* 104 in the *N*-methyl isomers and *m/z* 90 in the demethyl isomers) is useful to differentiate the two structural types. The third major fragment gives *m/z* 58 in the methylated isomers and *m/z* 44 in demethyltrewiasine. Presumably this fragment

TABLE 3. Ms/ms Daughters of $(MH\text{-}a)^+$ of Maytansinoids

| | Compound | Parent $(MH\text{-}a)^+$ | Daughters | | Others |
|---|---|---|---|---|---|
| | | | $(MH\text{-}a\text{-}b)^+$ | $(bH\text{-}18)^+$ | |
| **1** | maytansine | 631 | 486(40) | 128(100) | 504,454,100 |
| **2** | maytanprine | 645 | 486(13) | 142(100) | 504,454,114 |
| **3** | maytanbutine | 659 | 486(15) | 156(100) | 504,454,128 |
| **4** | maytanvaline | 673 | 486(9) | 170(100) | 504,454,142 |
| **5** | colubrinol | 675 | 502(15) | 156(100) | 128 |
| **6** | trewiasine | 689 | 516(21) | 156(100) | 484,128 |
| **7** | 10-epitrewiasine | 689 | 516(29) | 156(100) | 484,128 |
| **8** | dehydrotrewiasine | 687 | 516(50) | 154(100) | 484,128 |
| **9** | demethyltrewiasine | 675 | 516(100) | 142(12) | 534,484,502,222,114 |
| **10** | nortrewiasine | 675 | 502(40) | 156(100) | 470,128 |
| **14** | maytanacine | 546 | 486(100) | nd | 454 |

TABLE 4. Ms/ms Daughters of $(MH\text{-}a)^-$ of Maytansinoids

| Compound | Parent $(MH\text{-}a)^-$ | Daughters | | Others |
|---|---|---|---|---|
| | | $(b\text{-}H)^-$ | $(M\text{-}a\text{-}b)^-$ | |
| **1** maytansine | 630 | 144(100) | 485(15) | 594,467,449,180 |
| **2** maytanprine | 644 | 158(100) | 485(5) | 608,467,194 |
| **3** maytanbutine | 658 | 172(100) | 485(5) | 622,467,208 |
| **4** maytanvaline | 672 | 186(100) | 485(7) | 636,467,208 |
| **5** colubrinol | 674 | 172(100) | 501(12) | 639,606,465 |
| **6** trewiasine | 688 | 172(100) | 515(1) | 652,637,497,479,208 |
| **7** 10-epitrewiasine | 688 | 172(100) | 515(3) | 652,637,497,479,208 |
| **8** dehydrotrewiasine | 686 | 170(100) | 515(5) | 650,497,479,206 |
| **9** demethyltrewiasine | 674 | 158(100) | 515(2) | 638,623,497,479 |
| **10** nortrewiasine | 674 | 172(100) | 501(11) | 639,606,465 |
| **14** maytanacine | 545 | | 485(15) | |

also involves a proton transfer and comes from the fragment *m/z* 104 or 90 by loss of 46 Amu. Thus, side-chain positional isomers such as maytanprine (**2**) and demethyltrewiasine (**9**) are easily distinguished. By contrast, maytanbutine (**3**) and trewiasine (**6**) have identical side chains at *m/z* 174. These parents also have identical ms/ms daughter spectra confirming that the side-chain structures are identical.

TABLE 5. Ms/ms Daughters of Protonated C-3 Acid Side Chain

| Compound | Parent | Daughters |
|---|---|---|
| **1** maytansine | 146 | 104(100),58(85),43(30) |
| **2** maytanprine | 160 | 104(100),58(37),57(60) |
| **9** demethyltrewiasine | 160 | 90(40),71(100),43(75),44(19) |
| **8** dehydrotrewiasine | 172 | 126(12),102(8),69(100),58(35),41(9) |
| **3** maytanbutine | 174 | 104(100),71(75),58(40),43(30) |
| **6** trewiasine | 174 | 104(100),71(75),58(42),43(43) |
| **5** maytanvaline | 188 | 104(100),85(50),57(21),58(19) |

Daughter fragments of the acyl ion from the C-3 side chain show an ion 28 daltons less than the parent, which probably arises from loss of a carbonyl group. The other major daughter fragments come from cleavage between the nitrogen and the carbonyl, to form the acyl ion, and cleavage on the other side of the carbonyl to form a hydrocarbon fragment.

Ms/ms experiments are especially useful for the analysis of mixtures or to verify the presence of minor maytansinoids in partially purified samples. For example, both the

TABLE 6. Ms/ms Daughters of the C-3 Acyl Side Chain

| Compound | Parent | Daughters |
|---|---|---|
| **1** maytansine | 128 | 100(35),58(72),43(15) |
| **2** maytanprine | 142 | 114(32),58(76),57(20) |
| **9** demethyltrewiasine | 142 | 114(15),73(18),71(11),70(80),55(15), 44(12),43(31),29(10) |
| **8** dehydrotrewiasine | 154 | 126(40),69(90),41(9) |
| **3** maytanbutine | 156 | 141(6),128(22),83(5),71(26),58(66), 43(15) |
| **6** trewiasine | 156 | 141(9),128(24),83(8),71(30),58(80), 43(16) |
| **4** maytanvaline | 170 | 142(11),127(9),85(25),58(52),57(11) |

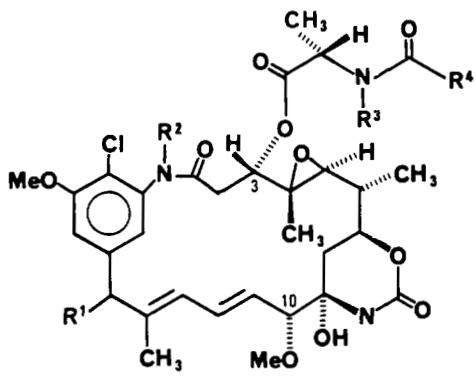

**1** $R^1$=H, $R^2$=$R^3$=$CH_3$, $R^4$=$CH_3$
**2** $R^1$=H, $R^2$=$R^3$=$CH_3$, $R^4$=$CH_2CH_3$
**3** $R^1$=H, $R^2$=$R^3$=$CH_3$, $R^4$=$CH(CH_3)_2$
**4** $R^1$=H, $R^2$=$R^3$=$CH_3$, $R^4$=$CH_2CH(CH_3)_2$
**5** $R^1$=OH, $R^2$=$R^3$=$CH_3$, $R^4$=$CH(CH_3)_2$
**6** $R^1$=$OCH_3$, $R^2$=$R^3$=$CH_3$, $R^4$=$CH(CH_3)_2$
**7** C-10 epimer of 6
**8** $R^1$=$OCH_3$, $R^2$=$R^3$=$CH_3$, $R^4$=$C(CH_3)$=$CH_2$
**9** $R^1$=$OCH_3$, $R^2$=$CH_3$, $R^3$=H, $R^4$=$CH(CH_3)_2$
**10** $R^1$=$OCH_3$, $R^2$=H, $R^3$=$CH_3$, $R^4$=$CH(CH_3)_2$
**18** $R^1$=H, $R^2$=$R^3$=$CH_3$, $R^4$=$C_5H_9$
**19** $R^1$=H, $R^2$=$R^3$=$CH_3$, $R^4$=$C_4H_7$
**20** $R^1$=H, $R^2$=$R^3$=$CH_3$, $R^4$=$C_6H_5$

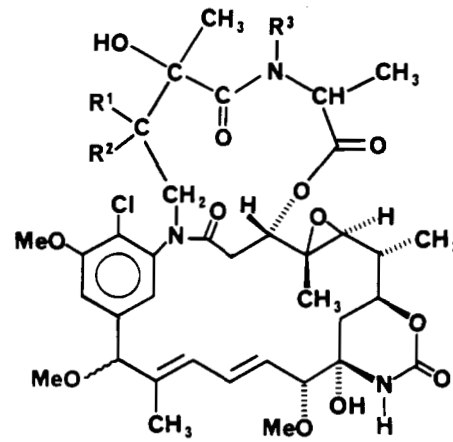

**11** $R^1$=$R^2$=$R^3$=H
**12** $R^1$=OH, $R^2$=$R^3$=H
**13** $R^1$+$R^2$=O, $R^3$=$CH_3$

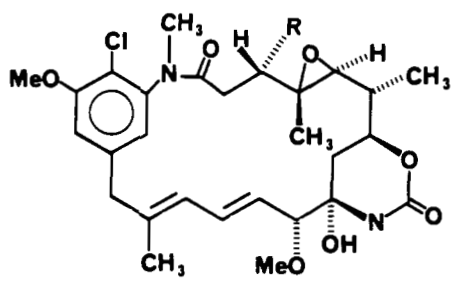

**14** R=$COCH_3$
**15** R=$COCH_2CH_3$
**16** R=$COCH(CH_3)_2$
**17** R=$COCH_2CH(CH_3)_2$

positive and negative ci spectra of our reference sample of maytanvaline (**4**) had indications of minor maytansinoid impurities that were previously undetected. In the positive ci spectrum, two additional ions having masses in the $(MH\text{-}a)^+$ region were observed. Extra fragments are not usually observed with masses in this area of the ci spectra of pure maytansinoids. Each ion was about 10% of the abundance of the *m/z* 673 ion, and each had an isotope pattern consistent with a molecule containing a chlorine atom. Fragment ions at *m/z* 685 and 707 were indicative of maytansinoids (**18**,**20**) with unknown side chains at C-3. To investigate this possibility, ms/ms daughters were scanned for the ions at *m/z* 673, 685, and 707. All three parents showed only two abundant daughters, a $(MH\text{-}a\text{-}b)^+$ daughter at *m/z* 486 indicating a normal maytansine ring system and a $(bH\text{-}18)^+$ daughter (at *m/z* 170 for the *m/z* 673 parent; at *m/z* 182 for the *m/z* 685 parent; and at *m/z* 204 in the *m/z* 707 parent). The tentative assignments of the *m/z* 685 and 707 parents were confirmed by ms/ms daughter scans on the ion 2 daltons higher, which would be expected to carry a $Cl_{37}$ isotope or 2 $C_{13}$ isotopes. Daughters

were seen at *m/z* 488 and 486 in the expected ratios (about 3:1). Daughters at *m/z* 182 and 184 mirrored the isotope ratios of the other daughter in the *m/z* 687 ms/ms scan, while these equivalent fragments were of *m/z* 204 and 206 in the *m/z* 709 daughter experiment.

Similarly, positive and negative ci spectra of the reference sample of maytanbutine (**3**) also showed evidence of an additional minor maytansinoid (**19**). A $(MH\text{-}a)^+$ signal at *m/z* 671 was observed in addition to the expected ion at *m/z* 658. The ms/ms daughter spectrum of the ion at *m/z* 671 revealed it was yet another previously undetected maytansinoid. This new compound contains one less methylene unit in the side chain than **18** because *m/z* 671 had daughters at *m/z* 486 and 168.

The structure of the side chains of these three new maytansinoids (**18**,**19**,**20**) was inferred from ms/ms daughter spectra of the expected fragments from the acyl ion of the side chains that were seen at *m/z* 168 in the maytanbutine sample and at *m/z* 182 and 204 in the maytanvaline sample. Daughters of *m/z* 204 were observed at *m/z* 91 and 119. These fragments indicate that the *m/z* 204 acyl ion has a phenyl side chain as $R_4$. This assignment was supported by the daughter spectrum of the ion at *m/z* 222, which had an abundant daughter at *m/z* 91. Phenyl substitution on the side chain in maytansinoids has not previously been reported.

The fragment of *m/z* 168 from the new compound found in the maytanbutine sample had daughters at *m/z* 140(20), 83(100), 58(50), and 55(8), while the protonated acid at *m/z* 186 had daughters at *m/z* 104(20), 83(100), 58(12), and 55(8). These daughter spectra indicate that $R_4$ of the side chain is $C_4H_7$. This side chain could either contain a double bond (like dehydrotrewiasine) or a cyclopropane ring like the minor isomer reported by Sneden *et al.* (8). Full characterization of these new compounds (**18**-**20**) was not accomplished because only small quantities of sample were available.

After the discovery of maytansinoids in higher plants, Japanese workers characterized a similar group of maytansinoids as components of the fermentation broth of *Nocardia* sp. (9), later renamed *Actinosynnema pretiosum* (10). These were esterified at C-3 with simple acids containing no nitrogen. Ms/ms experiments provide a convenient method of following the accumulation of these components during the fermentation. An aliquot of an EtOAc extract of the fermentation beer can be directly analyzed for these esters. Because positive and negative ci spectra have abundant $(MH\text{-}a)^+$ and $(M\text{-}a)^-$ ions to select for ms/ms experiments, usable full-scan ms/ms spectra can be obtained from low ng amounts of maytansinoid. Three daughter scans, sequentially selecting the $(MH\text{-}a)^+$ ion for ansamitocin P-2, P-3, and P-4 (*m/z* 560, 574, and 588) while the sample is heated in the ci source, all had the prominent daughter from the loss of the C-3 ester at *m/z* 486 as the base peak. Alternatively, it is simpler to do a single-parent experiment. This is accomplished by passing only the common daughter ion (*m/z* 486) through quadrupole Q3 while scanning Q1 normally. The resulting parent scan gives a spectrum of all parents that are separated by Q1 and undergo collisionally activated decomposition (cad) in the collision cell to a daughter at *m/z* 486. The relative yield of each parent ion corresponds to its abundance in the fermentation broth. Parents were observed at *m/z* 560 (ansamitocin P-2, **15**), 574 (ansamitocin P-3, **16**), and 588 (ansamitocin P-4, **17**). In the selected ion mode, selecting *m/z* 560, 574, or 588 as the parent and *m/z* 486 as the daughter, detection limits for the ansamitocins P-2, P-3, and P-4 in the low picogram range were obtained. Thus, analyzing 1-5 μl of a 1:1 EtOAc extract of the fermentation beer by ms/ms afforded detection in the low μg/liter range. The total levels of these three parents as measured in the ms/ms parent experiments correlated well with the toxicity measured by bioassay against *Filobasidium uniguttulatum* (11) as these compounds accumulated during the course of the fermentation.

## EXPERIMENTAL

REFERENCE MATERIALS.—Maytansine (**1**), maytanprine (**2**), maytanbutine (**3**), maytanvaline (**4**), and maytanacine (**14**) were gifts generously provided by Dr. A.T. Sneden, Virginia Commonwealth University, Richmond, Virginia. Compounds **5-13** were obtained from *Trewia nudiflora* as described previously (3). Reference samples of ansamitocins P-3 (**16**) and P-4 (**17**) were prepared by fermentation of *Actinosynnema pretiosum* ssp. *pretiosum* (syn. *Nocardia* sp.), NRRL B-16060, using procedures described previously (9).

INSTRUMENTATION.—All data were collected with a Finnigan MAT triple stage quadrupole mass spectrometer equipped with pulsed positive and negative ion chemical ionization and an INCOS data system. Isobutane was used as the reagent gas (0.25 torr). Argon was used as the target gas in cad experiments. The electron energy for ei and the ionization of the reagent gas plasma in ci was 70 eV and the source temperature was 140°. Samples were introduced via either the standard insertion probe or the direct exposure probe (in beam direct ci). Maytansinoids elute from the probe at temperatures in the range of 230-280°. Source pressures and collision cell pressures were measured by thermocouple gauges connected to the source and collision cell and are reported uncorrected. Data acquisition and mass spectrometer control were handled by the INCOS data system which controlled instrument scanning and mass setting parameters for the quadrupoles in ms and ms/ms experiments. Normal mass spectra were recorded by operating quadrupole Q1 and Q2 in the all pass mode (rf only) and scanning Q3. Daughter experiments were carried out by setting Q1 to pass only an ion of a selected *m/z* value. Q2 was used as a rf focusing collision cell at pressures in the range of $1\text{-}3\times10^{-3}$ torr, and a collision energy of 20 v, and Q3 was scanned normally. For parent experiments, Q3 was set to pass the daughter fragment of interest while Q1 was scanned.

## ACKNOWLEDGMENTS

Dr. David Labeda and Adolph Lagoda supplied beer from fermentation of *Actinosynnema pretiosum*, and compounds **16** and **17** were isolated from the beer by Barry Jones. Dr. Matthew Suffness, NCI, Bethesda, Maryland, also provided a reference sample of maytansine.

## LITERATURE CITED

1. Y. Komoda and T. Kishi, "Maytansinoids," in: "Anticancer Agents Based on Natural Product Models." Ed. by J.M. Cassady and J.D. Douros, Academic Press, New York, 1980, pp. 353, 389.
2. P.J. Reider and D.M. Roland, "The Maytansinoids," in: "The Alkaloids," Vol. 23. Ed. by A. Brossi, Academic Press, New York, 1984, pp. 71-156.
3. C.R. Smith and R.G. Powell, "Chemistry and Pharmacology of the Maytansinoid Alkaloids," in: "Alkaloids: Chemical and Biological Perspectives," Vol. 2. Ed. by S. William Pelletier, Wiley and Sons, 1984, pp. 149-205.
4. R.G. Powell, C.R. Smith, Jr., R.D. Plattner, and B.E. Jones, *J. Nat. Prod.*, **46**, 660 (1983).
5. R.A. Rousch and R.G. Cooks, *J. Nat. Prod.*, **47**, 197 (1984).
6. F.W. McLafferty, *Science*, **214**, 280 (1981).
7. R.G. Cooks, K.L. Busch, and G.L. Glish, *Science*, **222**, 273 (1983).
8. A.T. Sneden, W.C. Sumner, and S.M. Kupchan, *J. Nat. Prod.*, **45**, 624 (1982).
9. M. Asai, E. Mizuta, M. Izawa, K. Haibara, and T. Kishi, *Tetrahedron*, **35**, 1079 (1975).
10. T. Hasegawa, S. Tanida, K. Hatano, E. Higashide, and M. Yoneda, *Int. J. Syst. Bacteriol.*, **33**, 314 (1983).
11. K. Hatano, E. Higashide, and M. Yoneda, *Agric. Biol. Chem.*, **48**, 1889 (1984).

*Received 14 November 1985*